Quench-induced Dynamic Breakdown Strength of Liquid Helium for Superconducting Coils

S.Chigusa, N.Hayakawa, *Member, IEEE* and H.Okubo, *Member, IEEE*

***Abstract*—In this paper, we measured quench-induced dynamic breakdown strength of liquid helium (LHe) under various quench environment of superconducting (SC) coils for electrical insulation design of SC power equipment. Experimental results revealed that the dynamic breakdown strength of LHe drastically decreased with even small post-quench thermal energy of SC coils. However, the dynamic breakdown strength was improved with the increase in the pressure of LHe because of the suppression of thermal bubble disturbance in LHe. Moreover, we established 3-dimensional diagrams of the dynamic breakdown strength of LHe as a function of effective post-quench thermal energy density and pressure of LHe. The diagrams are applicable to the practical insulation design of SC equipment under quench environment.**

***Index terms*—quench, breakdown strength, insulation design**

I. Introduction

SC technology has great potential of a breakthrough in electric power system for next generation. Recently, developments of SC power equipment are stepping up to practical stages and suggest the trend of higher voltage operation such as several tens or hundreds of kV [1]-[3]. Therefore, it has been recognized that electrical insulation technology under cryogenic environment is essential for practical design of SC equipment. From this viewpoint, "Special Issue on Electrical Insulation in Superconducting Power Apparatus" was published in *Cryogenics* [4]. However, useful data for practical insulation design have not been obtained enough. Especially, for SC fault current limiters which make effective use of quench phenomena, dielectric performance under quench environment is one of the most important problems.

From the above viewpoints, we have been studying breakdown characteristics of LHe under quench environment. Breakdown characteristics of LHe with and without taking account of quench phenomena are named as "dynamic" and "static" breakdown characteristics, respectively [5],[6]. In this paper, we measured static and dynamic breakdown strength of LHe under various post-quench thermal energy, pressure of LHe and gap length. Experimental results revealed that insulation performance of SC coils was drastically reduced by quench-induced thermal bubble disturbance in LHe. Moreover, we obtained 3-dimensional diagram of dynamic breakdown strength of LHe for practical insulation design of SC equipment.

Department of Electrical Engineering, Nagoya University, Furo-cho, Chikusa-ku, Nagoya 464-8603, JAPAN.

II. Experimental

Figure 1 shows an SC coil - plane electrode system for the measurement of quench-induced dynamic breakdown characteristics of LHe. The SC coil had a flat configuration so as to make uniform electric field distribution in the gap space. Voltage taps arranged on the SC coil enabled us to detect the quench inception and propagation characteristics in the SC coil. The plane electrode was made of stainless steel and placed in parallel above the SC coil. The post-quench thermal energy of the SC coils can be controlled by using different types of SC wires as well as by changing prospective current levels as listed in TABLE I. Note that we evaluated the quench-induced thermal bubble disturbance in LHe as the effective post-quench thermal energy density J_{eff} [J/cm], as will be described in the next section.

Figure 2 shows the experimental setup composed of a large-current source including the SC coil, and a high-voltage source including the plane electrode. A high ac voltage of 60Hz below a static breakdown level of LHe was applied to the plane electrode for a given gap length. Under this condition, a large ac current of 60 Hz during only 1cycle caused the quench of SC coil, resulting in the generation of thermal bubble disturbance in LHe, which could induce the "dynamic" breakdown of the gap space.

The "dynamic" breakdown voltage V_d was defined as the minimum value of the applied voltage below which the breakdown was no longer induced by the quench of SC coil. On the other hand, the "static" breakdown voltage V_s was measured by gradually increasing the applied ac voltage V_{ac} at a rate of $1kV_{rms}$/sec without current flowing in the

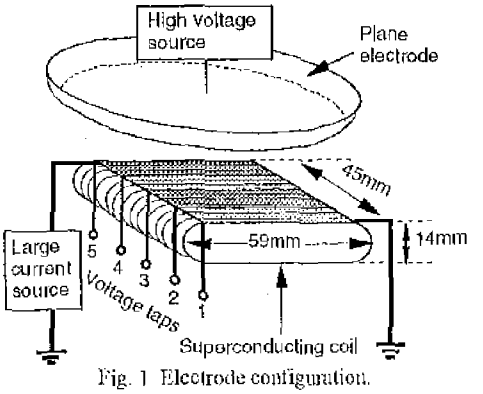

Fig. 1 Electrode configuration.

1051-8223/00$10.00

TABLE I Specifications of superconductors

	CuNi:Cu:NbTi	Diameter (stranded wire)	Quench current I_q (peak value)	Prospective current I_{pro} (peak value)	Length	Effective post-quench thermal energy density J_{eff} (1 cycle)
#1	2.1 : 0 : 1	0.5mm	70A	110A	12.5m	0.05J/cm
#2	4.0 : 0 : 1	0.9mm	140A	190A	7.0m	0.13J/cm
#3			190A	260A	7.0m	0.22J/cm

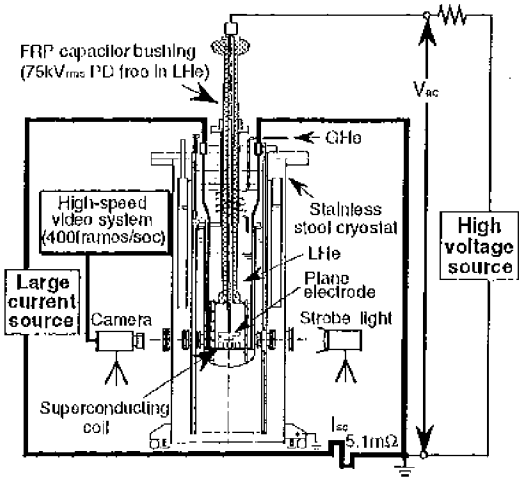

Fig. 2 Experimental setup.

coil. The static and dynamic breakdown strength E_s and E_d were calculated as the values of V_s and V_d divided by the gap length, all of which were designated by the peak values.

Investigation of breakdown characteristics was performed under various effective post-quench thermal energy density (J_{eff}=0.05-0.22J/cm), gap length (g=5-11mm) and pressure of LHe (P=0.1-0.2MPa). Simultaneously, thermal bubble behavior and dynamic breakdown in LHe were observed by using a high-speed video camera system (400frames/sec).

III. Results and Discussion

A. Quench-induced Dynamic Breakdown Phenomena

Figure 3(a) shows the time evolution of the current I_{sc}, voltage V_{sc} and resistance R_{sc} in each region of SC coil #2 for V_{ac}=31kV$_{peak}$, g=9mm and P=0.1MPa. The quench of #2 occurred when I_{sc}=140A, and V_{sc} and R_{sc} emerged at first between Tap3 and Tap4 (hereinafter Tap3-4) and the normal zone propagated in the neighboring Tap4-5 with the smaller magnitude than those in Tap3-4. No resistance appeared in the other regions Tap1-2 and 2-3. Figure 3(b) shows injected power W_{sc}, post-quench thermal energy J_{sc} and applied ac voltage V_{ac}. W_{sc} and J_{sc} were injected at first in the quench-initiated region Tap3-4. At 60ms after the quench-onset, V_{ac} abruptly collapsed, which means that the dynamic breakdown was induced.

Figure 4 shows the photographs of thermal bubble behavior and the quench-induced dynamic breakdown in the

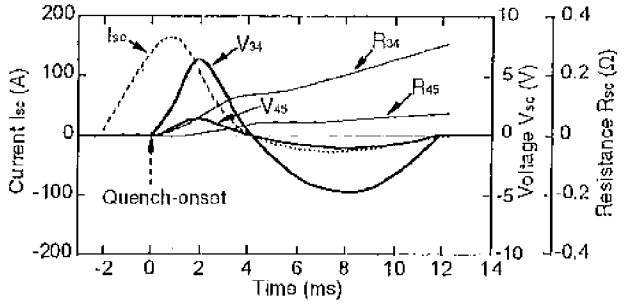

(a) Current I_{sc}, voltage V_{sc} and resistance R_{sc}

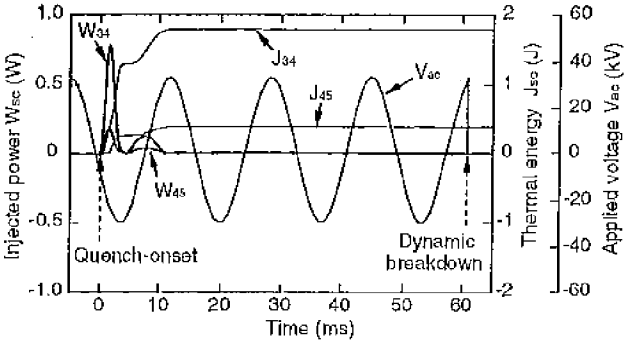

(b) Injected power W_{sc}, thermal energy J_{sc} and applied voltage V_{ac}

Fig. 3 Typical waveforms of quench and dynamic breakdown in SC coil #2 (V_{ac}=31kV$_{peak}$, g=9mm, P=0.1MPa).

case of Fig. 3. At 10ms after the quench-onset, a thermal bubble cluster was generated in Tap3-4, which corresponded to the quench-initiated region in Fig. 3. The bubble cluster was developed and propagated into the gap space, resulting in the thermal bubble disturbance in LHe. Finally, at 60ms after the quench-onset, a blight discharge path of dynamic breakdown was observed in the bubble disturbance. These results verify that the insulation performance of LHe was degraded by the quench of SC coil.

B. Dynamic Breakdown Strength of LHe

As was shown in Fig. 4, quench-induced bubble disturbance was developed on the SC coil and induced the dynamic breakdown. Thus, in order to evaluate the dynamic breakdown characteristics, it is necessary to take into account the contribution of bubble generation from adjacent SC windings. From this viewpoint, we introduced a parameter J_{eff} : effective post-quench thermal energy density. J_{eff} was defined as the following equation:

$$J_{eff} = k \cdot \frac{J_{sc}}{L} \quad [J/cm],$$

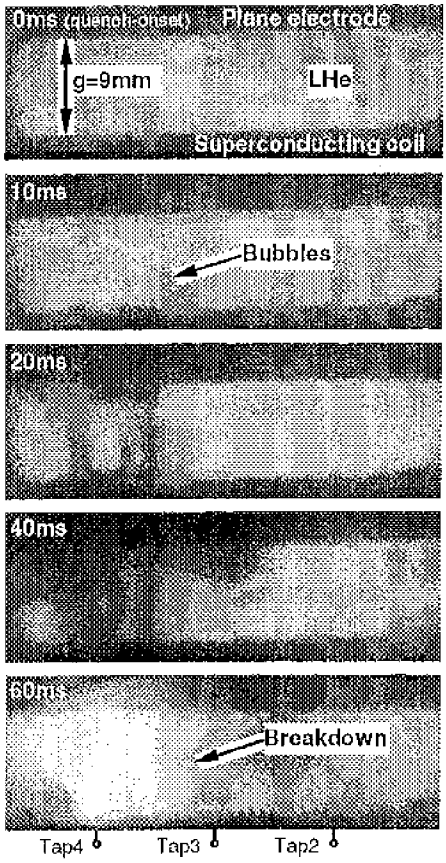

Fig. 4 Thermal bubble behavior and dynamic breakdown of LHe in the case of Fig. 3.

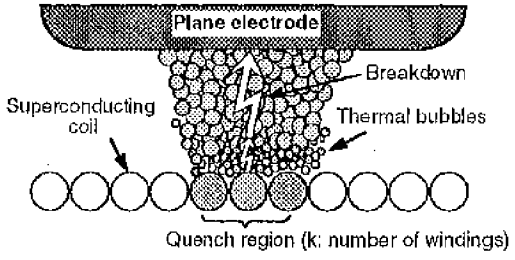

Fig. 5 Schematic illustration of thermal bubbles induced by quench of SC coil.

where J_{se} is the post-quench thermal energy accumulated during the quench period. k is the number of windings as illustrated in Fig. 5. L is the length of SC wire. k and L are defined as those in the quench region. In other words, J_{eff} is the thermal energy density per unit length of SC wire where thermal bubbles would be generated.

Figure 6 shows the static and dynamic breakdown strength E_s, E_d of LHe as a function of gap length at P=0.1MPa for different J_{eff}. As shown in Fig. 6, E_s is slightly reduced with the enlargement of gap length due to the size effect [1]. E_d is much smaller than E_s and slightly improved with the gap length, because the quench-induced thermal bubble disturbance would be relatively suppressed in the larger gap space. Figure 7 shows E_s and E_d as a

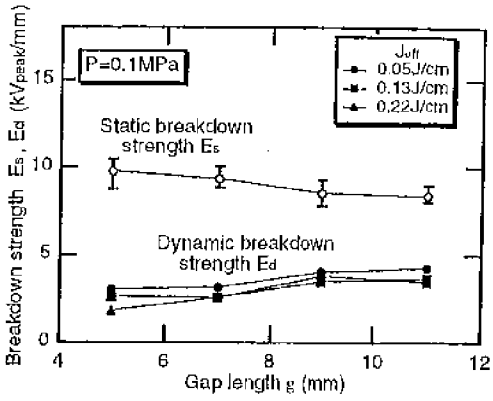

Fig. 6 Static and dynamic breakdown strength E_s, E_d of LHe as a function of gap length for P=0.1MPa.

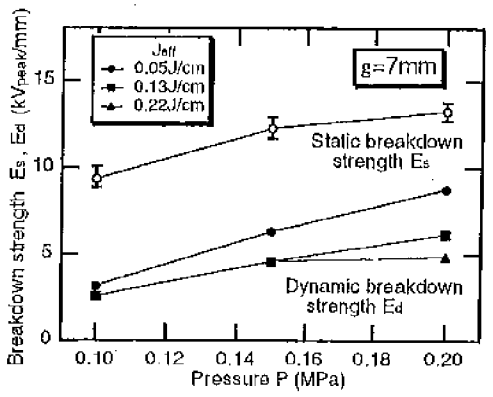

Fig. 7 Static and dynamic breakdown strength E_s, E_d of LHe as a function of pressure for g=7mm.

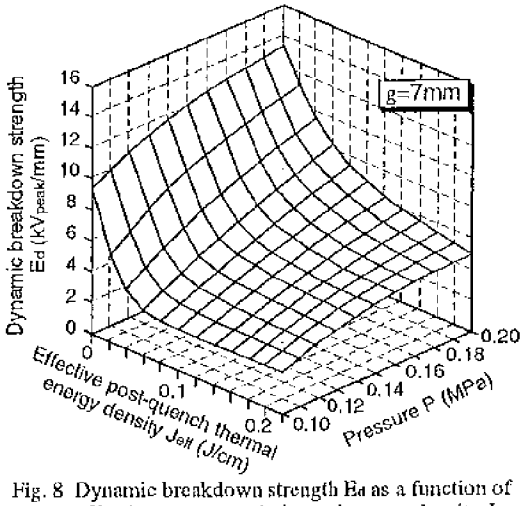

Fig. 8 Dynamic breakdown strength E_d as a function of effective post-quench thermal energy density J_{eff} and pressure P of LHe.

function of pressure of LHe at g=7mm. E_s and E_d are improved with pressure, since the pressurization of LHe suppresses the generation of thermal bubbles and increases the gaseous density in thermal bubbles. However, E_d decreases with the increase in J_{eff} due to the activated thermal bubble disturbance.

From these figures, we systematized the dynamic breakdown characteristics of LHe as the 3-dimensional diagram in Fig. 8, where E_d is evaluated as a function of J_{eff} and P at g=7mm. In this figure, E_d at J_{eff}=0J/cm corresponds to E_s. This diagram makes clear the drastic reduction of E_d with even small J_{eff} under uniform electric field distribution. The diagrams at the other gap lengths were similar to Fig. 8, because E_d was almost independent of the gap length, as was shown in Fig. 6.

C. Electrical Insulation Design for SC Equipment

For the practical insulation design of SC equipment, the combination of gap length and pressure of LHe should be optimized to avoid the dynamic breakdown even under quench environment. Figure 9 shows the 3-dimensional diagram of V_d as a function of J_{eff} and g at P=0.1MPa. For a given J_{eff}, V_d increases linearly with the increase in gap length, because the gap length dependence of E_d is small. Similar diagrams for different pressures

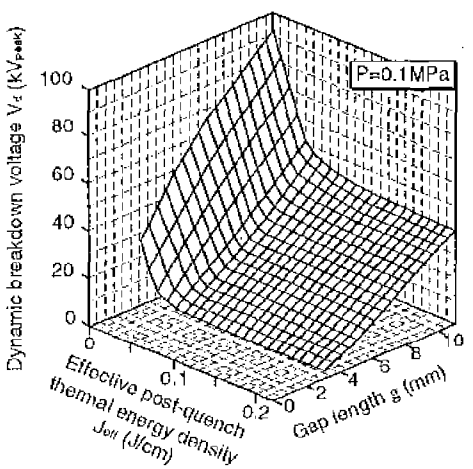

Fig. 9 Dynamic breakdown voltage V_d of LHe as a function of effective post-quench thermal energy density J_{eff} and gap length g for P=0.1MPa.

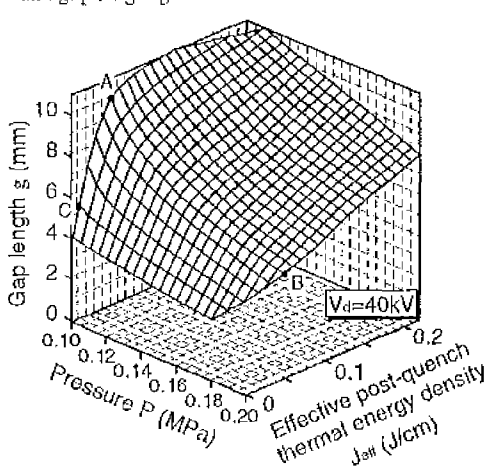

Fig. 10 Equi-breakdown voltage surface of LHe as a function of effective post-quench thermal energy density J_{eff}, gap length g and pressure P of LHe for V_d=40kV.

can be also obtained. From these diagrams, we can derive the equi-breakdown voltage surface for e.g. V_d=40kV as a function of J_{eff}, g and P, as shown in Fig. 10. This diagram can be utilized as follows: If J_{eff} is given as 0.05J/cm, g=10mm is required at P=0.1MPa (point A). However, when the pressure of LHe can be raised up to 0.2MPa, the gap length may be reduced to 5mm (point B). Moreover, in the case of smaller J_{eff} as 0.01J/cm, g=5mm can be applicable even at P=0.1MPa (point C). Similar diagrams for different V_d can be also derived from Fig. 9. From these equi-breakdown voltage diagrams, we can optimize the combination of gap length and pressure of LHe under arbitrary J_{eff} for practical and efficient insulation design of SC equipment.

IV. Conclusions

In this paper, we investigated static and dynamic breakdown characteristics of LHe for SC coil - plane electrode system under various effective post-quench thermal energy density J_{eff}, gap length g and pressure P of LHe. Experimental results are summarized as follows.

1. Quench of SC coil could induce dynamic breakdown in thermal bubble disturbance in LHe.
2. Dynamic breakdown strength E_d of LHe was drastically reduced with even small J_{eff} under uniform electric field distribution.
3. 3-dimensional diagram of E_d was established as a function of J_{eff} and P.
4. Equi-breakdown voltage surface diagram was derived as a function of J_{eff}, g and P, which would contribute to the practical and efficient insulation design of SC equipment.

References

[1] H.Okubo, M.Hikita, H.Goshima, H.Sakakibara, N.Hayakawa, "High Voltage Insulation Performance of Cryogenic Liquids for Superconducting Power Apparatus", *IEEE Trans. on Power Delivery*, Vol.11, No.3, pp.1400-1406, 1996.

[2] T.Verhaege, C.Cottevieille, P.Estop, J.P.Tavergnier, M.Bekhaled, C.Bencharab, P.Bonnet, Y.Laumond, V.D.Pham, C.Ponmarede, P.G.Therond, "Experiments with a High Voltage (40kV) Superconducting Fault Current Limiter", *Cryogenics*, Vol.36, No.7, pp.521-526, 1996.

[3] P.L.Fadie, M.Nassi, S.R.Norman, P.Caracino, M.Covoet, C.Boisseau, P.F.Sirot, "Pirelli-EDF Development on Superconducting Cables", *Proc. of Jicable*, pp.103-108, 1999.

[4] J.Gerhold and M.Hara, "Special Issue on Electrical Insulation in Superconducting Power Apparatus", *Cryogenics*, Vol.38, No.11, 1998.

[5] S.Chigusa, Y.Taniguchi, N.Hayakawa, H.Okubo, "Influence of Quench-induced Thermal Bubble Disturbance on Insulation Performance of Liquid Helium for Superconducting Power Apparatus", *Cryogenics*, Vol.38, No.9, pp.931-936, 1998.

[6] S.Chigusa, H.Maeda, Y.Taniguchi, N.Hayakawa, H.Okubo, "Insulation Performance of Pressurized Liquid Helium under Quench-induced Thermal Bubbles Disturbance", *IEEE Trans. on Dielectrics and Electrical Insulation*, Vol.6, No.3, pp.385-392, 1999.